FULL PAPER

Dalton
www.rsc.org/dalton

Limonene-derived phosphines in the cobalt-catalysed hydroformylation of alkenes

Anastasios Polas,†[a] James D. E. T. Wilton-Ely,[a] Alexandra M. Z. Slawin,[a] Douglas F. Foster,†[b] Petrus J. Steynberg,[c] Michael J. Green[c] and David J. Cole-Hamilton*[a]

[a] *School of Chemistry, University of St. Andrews, St. Andrews, Fife, Scotland, UK KY16 9ST. E-mail: djc@st-and.ac.uk; Fax: +44-(0)1334-463808; Tel: +44-(0)1334-463805*

[b] *Catalyst Evaluation and Optimisation Service, School of Chemistry, University of St. Andrews, St. Andrews, Fife, Scotland, UK KY16 9ST*

[c] *Research and Development, Sasol Technology (Pty) Ltd., P.O. Box 1, Sasolburg, 1974, South Africa*

Received 26th August 2003, Accepted 16th October 2003
First published as an Advance Article on the web 11th November 2003

Cobalt complexes involved in the hydroformylation of alkenes using (4*R,S*)-4,8-dimethyl-2-octadecyl-2-phosphabicyclo[3.3.1]nonane (LIM-18), which consists of a mixture of two diastereomers, have been studied. Complexation to cobalt has been used to separate or enrich the enantiomers so that spectroscopic parameters can be determined for complexes of the form $[Co_2(CO)_{8-n}(LIM\text{-}18)_n]$ (n = 1 or 2) and $[Co(CO)_3(LIM\text{-}18)_2][Co(CO)_4]$ containing the different diastereomers. An X-ray structure of a complex of the form $[Co(CO)_3(LIM\text{-}18)]_2$ shows it to contain the (4*R*) isomer, but since this was isolated from a mixed solution of diastereomers, this does not definitively identify whether the (4*R*) or (4*S*) isomer is the more strongly coordinating isomer. Experimental studies backed up with molecular modelling suggest that steric and electronic effects determine which isomer reacts preferentially in coordination, protonation and methylation reactions. The (4*R*) isomer is the more strongly coordinating and is metallated preferentially, although the (4*S*) isomer is the more basic. Variable temperature and high pressure NMR studies on the acyl complex, $[Co(C(O)C_5H_9)(CO)_3(LIM\text{-}18)]$, suggest that product elimination may be accompanied by isomerisation to branched acyl species. Modified cobalt catalysed hydroformylation of reactions suggest that the two diastereomers of LIM-18 do not give greatly different rates or selectivities and that a long chain secondary alkyl substituent on the LIM gives lower linear selectivity and a faster rate than LIM-18. LIM-Bu^t gives a selectivity similar to that obtained using LIM-18.

Introduction

The hydroformylation of alkenes is one of the great successes of industrial homogeneous catalysis. For short chain alkenes, rhodium catalysts modified with triphenylphosphine are used because of their high activity under mild conditions and their good selectivity towards the linear product aldehyde.[1,2] However, for long chain alkenes, which give long chain aldehydes for use in the manufacture of plasticisers, soaps and detergents, these catalysts have not been used because they decompose at the temperatures required for the separation of the product from the catalyst by distillation. A pilot plant employing low temperature distillation is currently under commissioning at Sasol in South Africa, however.

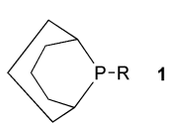

1

Because of the potential problems of catalyst decomposition during the product separation, all commercial plants for long chain aldehydes and alcohols currently use cobalt based technology.[1] Some systems use $[Co_2(CO)_8]$ as the catalyst precursor, in which case the products are aldehydes, the selectivity to the desired linear aldehyde is low and the reaction conditions are very harsh (300 bar, 200 °C). In other plants, tertiary phosphines are used to modify the cobalt based catalysts, with the result that better linear selectivities can be obtained (up to 10 : 1 linear : branched (l : b) ratio with ligands such as **1**), much milder conditions are applied (90 bar, 200 °C) and alcohols are formed instead of aldehydes.[3] Since alcohols are generally desired, this is an advantage, but the hydrogenation activity means that some alkene is usually lost through hydrogenation to alkane.

The greatest advantage cobalt catalysts have is their increased selectivity for linear alcohols specifically when using mixtures of internal and terminal alkenes produced in the Shell Higher Olefin Process developed in the 1960s.[4] Existing technology and infrastructure for hydroformylation under high pressure and temperature, combined with the stability of cobalt catalysts towards poisons, allowing for lower grades of feedstock, has also contributed to the continued use of cobalt catalytic systems by petrochemical giants such as Exxon, Shell, CdF Chimie, Nissan and BASF for the industrial formation of 'fatty alcohols'.

Compound **1** is derived from the addition of a primary phosphine across cycloocta-1,5-diene, but two regioisomers can be formed and these are relatively difficult to separate.[5] In this paper, we report some studies of a cobalt system modified with a phosphine formally derived in a similar way, but from (*R*)-(+)-limonene. Detailed results of the use of this ligand in cobalt catalysed hydroformylation reactions have been patented[6] and a recent publication reports that the chain length of the alkyl group on phosphorus has a marked effect on the activity and selectivity of the hydroformylation reaction.[7] Increasing the chain length increases the reaction rate, but decreases the linear selectivity and extent of alkene hydrogenation. By using high pressure spectroscopy and molecular modelling, these changes have been attributed to steric effects leading to a greater proportion of the cobalt catalyst being unmodified (no coordination of P ligand) for the longer chain alkyl phosphines. The unmodified system gives higher rates but lower selectivities and less competing alkene hydrogenation.[7]

† Current address: Sasol Technology (UK) Ltd., Purdie Building, North Haugh, St. Andrews, Fife, Scotland, UK KY16 9ST.

DOI: 10.1039/b310233e

Results and discussion

Ligand synthesis and separation of the diasteroisomers

The sterically demanding ligand (4-*R,S*)-4,8-dimethyl-2-octadecyl-2-phospha-bicyclo[3.3.1]nonane (LIM-18) **2** (see Scheme 1) is derived from the procedure recently reported by Robertson *et al.*[8] where phosphine (PH_3) is reacted with (*R*)-(+)-limonene in the presence of a radical initiator. The formed bicyclic secondary phosphine **3** is then reacted with 1-octadecene and the anti-Markovnikov radical addition ensues. The resulting product is a 55:45 mixture of two diastereomers exhibiting resonances at δ −45.2 and −51.7 ppm in the ^{31}P NMR spectrum. Separation of the two diastereomers by conventional means (distillation, recrystallisation and chromatography) proved both difficult and unsuccessful partly because of oxidation of the phosphine and partly because the long C_{18} tail makes the physical properties of the diastereomers very similar. However, on reaction of an excess of the phosphine with $[Co_2(CO)_8]$, one diastereomer was found to complex preferentially. Surprisingly, the diastereomer resonating at δ −45.2 ppm (LIM-18A) was more strongly coordinating, even though the greater shielding of the P atom in the other isomer δ −51.7 (LIM-18B) suggests it is the more basic diastereomer. This is supported by a protonation experiment in which the LIM-18B isomer reacts preferentially. Molecular modelling suggests that it is the (4*R*) isomer which resonates at δ −45.2[7] (see below). The preferential coordination of LIM-A can be used to separate the diastereomers.

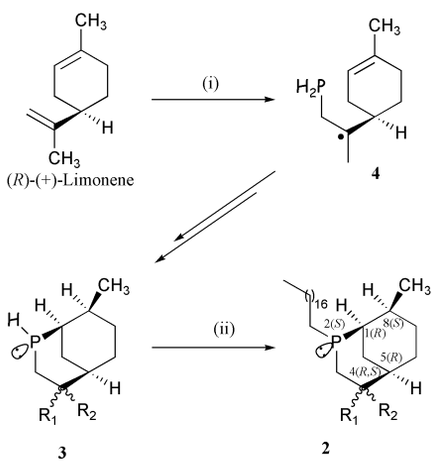

Scheme 1 Synthesis of ligand **2** from *R*-(+)-limonene and PH_3. (i) PH_3 + initiator, (ii) 1-octadecene + initiator.

Reaction of LIM-18 with $[Co_2(CO)_8]$ in light petroleum leads to the precipitation of an oil, identified by comparison of its spectroscopic properties with those of the PBu_3 analogue[9] as $[Co(LIM\text{-}18)_2(CO)_3][Co(CO)_4]$. By employing a deficiency of LIM-18 (LIM-18:Co = 2:6) in this reaction, the oil contains 68% $[Co(LIM\text{-}18A)_2(CO)_3][Co(CO)_4]$, 29% $[Co(LIM\text{-}18A)(LIM\text{-}18B)(CO)_3][Co(CO)_4]$ and 3% $[Co(LIM\text{-}18B)_2(CO)_3][Co(CO)_4]$. Heating this oil in toluene converted it to predominantly $[Co_2(LIM\text{-}18A)_2(CO)_6]$. Alternatively, by using an excess of LIM-18 (LIM 18:Co = 6:4), removing the oil and eluting the supernatant liquid through a silica column (100% CH_2Cl_2 to remove the cobalt complexes formed and then 100% Et_2O to elute the ligand), a sample of ligand enriched in LIM-18B (>95%) was isolated.

The separation of the two diastereomers and their subsequent reactions with $[Co_2(CO)_8]$ allowed the definitive assignment of resonances observed in the ^{31}P NMR spectra of the complexes shown in Table 1. This was essential as up to twelve resonance peaks of varying intensity within 10 ppm can be observed in the ^{31}P NMR spectrum of some complexes made with unresolved LIM-18 due to differing products containing one or two phosphines. In the case of the bis-phosphine complexes, both phosphines can be the same or different diastereomers. If they are different, the P atoms are inequivalent and couple to one another.

Table 1 ^{31}P data for cobalt complexes of the two different diastereomers of LIM-18 in $CDCl_3$[a]

Complex	$^{31}P\{^1H\}$NMR ($CDCl_3$)
$[Co(CO)_3((4R)\text{-LIM-18})_2][Co(CO)_4]$	37.8
$[Co(CO)_3((4S)\text{-LIM-18})_2][Co(CO)_4]$	40.6
$[Co(CO)_3((4R,S)\text{-LIM-18})_2][Co(CO)_4]$	37.9 (d, $^2J_{P-P}$ = 65 Hz)
	40.5 (d, $^2J_{P-P}$ = 65 Hz)
$[Co(CO)_3((4R)\text{-LIM-18})]_2$	37.9
$[Co(CO)_3((4S)\text{-LIM-18})]_2$	40.4
$[Co(CO)_3((4R,S)\text{-LIM-18})]_2$	37.6 (d, $^3J_{P-P}$ = 13 Hz)
	40.4 (d, $^3J_{P-P}$ = 13 Hz)
$Co_2(CO)_7((4R)\text{-LIM-18})$	41.4
$Co_2(CO)_7((4S)\text{-LIM-18})$	44.0
(4*R*)-LIM-18	−45.2
(4*S*)-LIM-18	−51.7
(4*R*)-LIM-18-oxide	45.5
(4*S*)-LIM-18-oxide	47.4

[a] The assignments to (4-*R*) and (4-*S*) assume that LIM-18A is (4-*R*) and LIM-18B is (4-*S*) (see text). The same assignment was made in ref. 7.

Attempted determination of the absolute stereochemistry of the different diastereomers

It has previously been shown[8] that the two diastereomers arise from an indiscriminate H addition to the tertiary carbon radical of **4** following addition of $H_2P^{\bullet}$ to the exocyclic double bond of limonene (see Scheme 1) and this is confirmed by the observation that deprotonation of the primary phosphine, **3**, with BuLi gives the phosphide anion, again as a mixture of two diastereomers (^{31}P NMR δ −128.6 and −142.6 ppm), thus ruling out the phosphorus atom as being the centre of chiral ambiguity. Subsequent radical additions must occur in a highly diastereoselective manner as only two out of a possible eight diastereomers were observed.[10] The high steric strain of the bicyclic phosphine was also observed to effect a stereoselective mode of attack in nucleophilic substitution reactions. Coupling the phosphide of this species to a long chain alkyl bromide again exhibited only two peaks (δ −36.1, −42.1 ppm) rather than the four expected if attack at the phosphorous were not diastereoselective. As all other atoms on the bicyclic ring are fixed, it is the orientation of the methyl group at the C_4 position of LIM-18 which determines both the stereoselective mode of attack and the ligating ability.

Crystals of $[Co(CO)_3(LIM\text{-}18)]_2$ were grown from a sample of the oil, $[Co(CO)_3(LIM\text{-}18)_2][Co(CO)_4]$ enriched in LIM-18A, on standing under an atmosphere of nitrogen. ^{31}P NMR analysis of the resulting crystals embedded in a waxy solid revealed a 68:29:3 mixture of the diastereomers with $[Co(CO)_3(LIM\text{-}18A)]_2$ in excess. A crystal was selected and found to be suitable for X-ray structure determination (Figs. 1 and 2, Table 2). Numbering of the ligand follows that of the phosphinic acid which was reported recently by Robertson *et al.*[8]

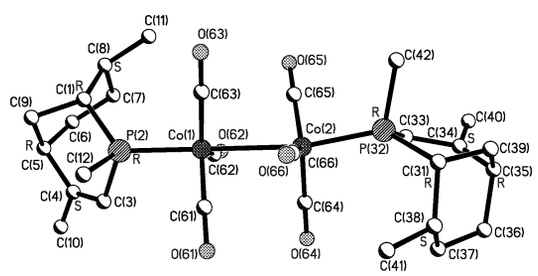

Fig. 1 X-ray crystal structure and numbering scheme for the core of $[Co_2(CO)_6(LIM\text{-}18)_2]$. The $C_{18}H_{37}$ chains have been omitted for clarity.

Table 2 Selected bond lengths (Å) and angles (°) for $[Co(CO)_3(PC_{28}H_{55})]_2$

Co(1)–Co(2)	2.6687(12)	C–O	1.115–1.233
Co(1)–P(2)	2.192(2)	Co(2)–P(32)	2.201(2)
Co(1)–C(61)	1.776(8)	Co(2)–C(64)	1.774(7)
Co(1)–C(62)	1.671(8)	Co(2)–C(65)	1.651(10)
Co(1)–C(63)	1.752(7)	Co(2)–C(66)	1.718(9)
P(2)–C(1)	1.865(8)	P(32)–C(31)	1.859(7)
P(2)–C(3)	1.677(11)	P(32)–C(33)	1.821(10)
P(2)–C(12)	1.654(2)	P(32)–C(42)	1.885(2)
P(2)–Co(1)–Co(2)	177.87(7)	P(32)–Co(2)–Co(1)	170.23(8)
P(2)–Co(1)–C(61)	94.7(3)	P(32)–Co(2)–C(64)	96.6(3)
P(2)–Co(1)–C(62)	95.8(3)	P(32)–Co(2)–C(65)	88.6(3)
P(2)–Co(1)–C(63)	94.7(2)	P(32)–Co(2)–C(66)	96.9(3)
Co(1)–P(2)–C(1)	124.9(3)	Co(2)–P(32)–C(31)	128.0(3)
Co(1)–P(2)–C(3)	114.8(4)	Co(2)–P(32)–C(33)	109.0(3)
Co(1)–P(2)–C(12)	115.12(11)	Co(2)–P(32)–C(42)	109.99(10)
C(1)–P(2)–C(3)	102.5(5)	C(31)–P(32)–C(33)	101.4(4)
C(1)–P(2)–C(12)	105.3(3)	C(31)–P(32)–C(42)	100.5(2)
C(3)–P(2)–C(12)	87.4(5)	C(33)–P(32)–C(42)	105.9(4)
C(61)–Co(1)–C(62)	114.2(4)	C(64)–Co(2)–C(65)	116.3(4)
C(61)–Co(1)–C(63)	117.3(4)	C(64)–Co(2)–C(66)	114.5(4)
C(62)–Co(1)–C(63)	126.1(4)	C(65)–Co(2)–C(66)	127.8(4)
O–C–Co	170–177		

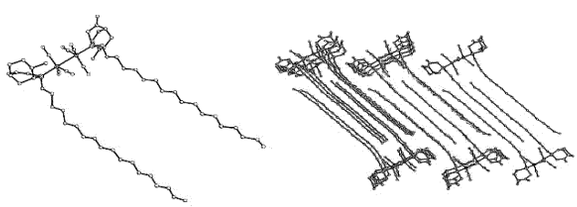

Fig. 2 Molecular structure and packing diagram for $[Co_2(CO)_6(LIM\text{-}18)_2]$.

Interesting features in the solid state structure of the dimer complex include alignment of the C_{18} hydrocarbon chains in the same plane. The chains interpenetrate to form flat sheets when packing (see Fig. 2). The structure of the complex is comparable with previous reported structures of $[Co(CO)_3L]_2$ where L is a monodentate ligand [11,12] although the ligands are not related by a C_2 axis (*i.e.* the PCoCoP backbone is not linear as is usually the case [11,12]). The need for the complex to adopt both a staggered arrangement and the flat sheet packing of the long hydrocarbon chains distorts the preferred linear alignment of the Co(1)–Co(2)–P(32) bond angle to 170° (*cf.* Co(2)–Co(1)–P(2), 178°). Also affected is a more acute C(3)–P(2)–C(12) angle of 87.4° compared to ~102° as observed on the P(32) ligand and other phosphine complexes. It is also in these ligand bonds that the greatest variance in atomic distance occurs (P(2)–C(12) is 0.23 Å shorter than P(32)–C(42)). These distortions probably arise from packing forces in the solid state. There is certainly no evidence for inequivalent P atoms in the ^{31}P NMR spectrum. Also, unlike the crystallisation of the phosphinic acid where the two diastereomeric pairs were incorporated into the crystal lattice,[8] the single crystal is seen to be diastereomerically pure. The C(5) atom was affixed with *R* configuration (from (*R*)-(+)-limonene), which also fits well with the predicted computational analysis of the diffraction pattern. All other chiral atoms were assigned from this point so that the ligand bound in this complex has the (1-*R*,4-*R*,5-*R*,8-*S*) configuration whilst the other stable diastereomer is (1-*R*,4-*S*,5-*R*,8-*S*). It should be noted that the *R* stereochemistry observed for the phosphorus atom P(2)/P(32) in the complex corresponds to the *S* configuration at P in the free phosphine. Also, atoms C8/C38 have *S* stereochemistry, as in both diastereomers of the phosphinic acid derived from the LIM skeleton.[8]

As the crystals were grown from an 82:17 mixed LIM-18A:LIM-18B diastereomeric complex solution, it is not possible definitively to confirm which of these is present in the crystalline complex, particularly as the crystal was accompanied by a waxy solid containing 68:29:3 $[Co(CO)_3(LIM\text{-}18A)]_2$:$[Co_2(CO)_6(LIM\text{-}18A)(LIM\text{-}18B)]$:$[Co(CO)_3(LIM\text{-}18B)]_2$. Some crystals were obtained from a different mixture containing essentially pure LIM-18B, but these did not diffract sufficiently for a structure solution.

Because of the problem of identifying unambiguously which diastereomer binds more readily to the cobalt and in order to try to determine to what extent the preferential binding of LIM-18A to cobalt depends upon steric or electronic effects, we extended our molecular modelling studies on the two ligands, their complexes, $[HCo(CO)_3(LIM\text{-}18)]$, their protonated forms and the products of their reactions with methyl triflate, as well as experimental studies of the protonation and methylation reactions. One of us has already reported that molecular modelling studies suggest that it is the (4*R*) isomer which binds preferentially in $[HCo(CO)_3(LIM\text{-}18)]$ and in a variety of other limonene derived phosphines bearing different alkyl substituents.[7]

Experimentally, LIM-18A reacts preferentially with Me^+ and $[Co_2(CO)_8]$. ^{31}P NMR studies show that the ratio of equilibrium constants for LIM-18A and LIM-18B is 1.4 for the reaction with methyl triflate whilst that for complexation with $[Co_2(CO)_8]$ is 7.0. Protonation of LIM-18A and LIM-18B with *p*-toluenesulfonic acid leads to very broad resonances in the ^{31}P NMR spectrum. This broadening effect increases with the amount of acid added but disappears once all phosphine has been protonated. This indicates that an exchange process is operating between protonated and non-protonated forms. Measuring the spectra at low temperature (0 °C) reduced the broadening dramatically and allowed accurate integration of the signals. It was observed that the LIM-18B isomer reacts preferentially with the acid, giving a value of 0.12 for the ratio of equilibrium constants for LIM-18A and LIM-18B. This suggests that the P atom in LIM-18B is slightly more basic than that in LIM-18A (an observation supported by the higher field chemical shift) ‡ and so preference is determined predominantly by electronic effects. The much greater preference for coordination of the less basic LIM-18A to cobalt suggests that steric effects dominate in that case. The preference for LIM-18A in the methylation experiment seems also to be directed by steric considerations, though the much lower value of 1.4 (compared to 7.0 for Co complexation) for the ratio of equilibrium constants indicates that steric factors play a lesser role.

‡ The P–H coupling constant in **3** (196 Hz) and the ν_{CO} values are identical for both isomers, so are not helpful in determining relative basicities of the two diasteriomers.

Table 3 Calculated heats of reaction (4*R*) or (4*S*)-LIM-18 with $[HCo(CO)_4]$ and of (4*R*) or (4*S*)-LIM-2 with H^+ (from H_3O^+)

LIM isomer	Reagent	ΔH_{react}/kJ mol^{-1}
(4-*R*)-LIM-18	$[HCo(CO)_4]$	−3.43[7]
(4-*S*)-LIM-18	$[HCo(CO)_4]$	9.37[7]
(4-*R*)-LIM-2	Me^+	176.81
(4-*S*)-LIM-2	Me^+	175.43
(4-*R*)-LIM-2	H^+	−300.83
(4-*S*)-LIM-2	H^+	−290.16

Based on calculated heats of reaction for the complexation reaction of the (4*R*) and (4*S*) LIM-18 diastereomers with $[HCo(CO)_4]$, the preferred isomer is (4*R*) (Table 3).[7] On this basis, we conclude that the (4*R*) isomer binds preferentially to cobalt and hence that the crystal selected for the X-ray structure determination contains the more strongly coordinating diastereomer.

An attempt was also made to correlate the observed experimental basicity differences (LIM-18A and LIM-18B) with theoretical values. From the data in Table 3 it can be seen that for the differences between the heats of reaction of the two diasteromers in protonation and methylation reactions are small relative to their absolute values, so meaningful conclusions cannot be drawn. The absolute accuracy of DFT quantum calculations is dependent on many factors: the choice of Hamiltonian, basis set used, the type of reaction and the reaction environment. The absolute energy errors are still large (~4–65 kJ mol^{-1}).[13] There are examples where the absolute energy accuracy (thermochemistry) is entering the < 4 kJ mol^{-1} domain.[14] Relative energy differences which are used in this paper are more accurate, however, arguments based on small energy differences relative to the absolute values (methylation and protonation reactions, Table 3) should always be treated cautiously. The energy values reported in Table 3 are total electronic energies at 0 K only. For the purpose of this theoretical study, thermodynamic properties (ΔG, ΔH and $T\Delta S$) of the said reactions were not calculated. Solvation effects were also not accounted for in the theoretical study and both of the latter are expected to impact on the calculated reactions energies specifically for the alkylation and protonation reations where charged species are involved. The energy differences observed for the complexation reactions are more significant and they suggest that the (4*R*) isomer coordinates preferentially, so we have assumed that LIM-18A is the (1-*R*,4-*R*,5-*R*,8-*S*) isomer.

High pressure NMR studies

In order to obtain spectroscopic parameters for other possible intermediates that may be observed under catalytic conditions, HP NMR studies were carried out on the hexanoyl complex, $[Co\{C(O)(CH_2)_4CH_3\}(CO)_3(LIM\text{-}18)]$ (**5**), which was prepared from the reaction of an equimolar amount of LIM-18 with a solution of the acyl(tetracarbonyl)cobalt complex preformed using known procedures.[15,16]

^{31}P NMR analysis in toluene under CO (1 bar) at room temperature (Fig. 3a) showed two resonances at 20.6 and 18.5 ppm which are assigned to the two diastereomers of the acyl species, **5** in Scheme 2. Also present were two sharp peaks at 44.7 and 42.1 ppm, which are assigned to the monophosphine substituted dimeric species $[Co_2(CO)_7(LIM\text{-}18)]$ (**6**) which have been prepared separately from the reaction of $[Co(CO)_3(LIM\text{-}18)]_2$ with $[Co_2(CO)_8]$ (see Experimental section and Table 1). The marginally different chemical shifts arise because of the different solvent used for the HPNMR studies. When the reaction was repeated using a 1:4 Co:L ratio, the $[Co(CO)_3(LIM\text{-}18)]_2$ dimers were preferentially formed with only a small amount of the acyl species being observed and no $[Co_2(CO)_7(LIM\text{-}18)]$.

The solution of terminal acyl complex, **5**, was transferred to a high pressure NMR cell, sealed and pressurised with syngas

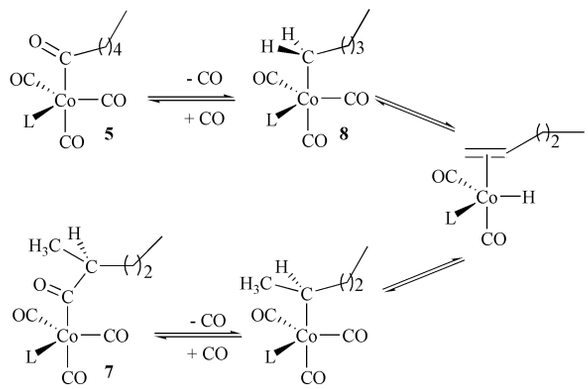

Scheme 2 Proposed mechanism of formation of branched acyl intermediates during high pressure NMR studies.

(1:1, 75 bar). The spectrum, at ambient temperature (Fig. 3b), shows the appearance of a small amount of the $[Co(CO)_3(LIM\text{-}18B)]_2$ resonating at 40.6 ppm, which was probably formed through oxidative addition of molecular hydrogen followed by reductive elimination of the aldehyde. A new peak observed at 21.0 ppm is thought to be from a LIM-18B branched acyl complex, **7**, rather than the LIM-18B terminal alkyl complex **8**, (see Scheme 2) because (i) the acyl complex is more stable than the alkyl and (ii) the alkyl complex would be expected to resonate much further upfield with respect to the acyl complex on the basis of relative chemical shifts from literature data for acyl/alkyl complex pairs.[1,2] On increasing the reaction temperature to 60 °C, (Fig. 3c) the amount of terminal acyl complex, **5**, decreases, resonances from both diastereomers of $[Co(CO)_3(LIM\text{-}18)]_2$ are observed and the predominant species are $[Co_2(CO)_7(LIM\text{-}18)]$. The resonance at 21 ppm (which shifts downfield with increasing temperature) increases along with a new species at 20.1 ppm. Assuming the species at 21 ppm is in fact the LIM-18B branched acyl complex, **7**, then this new species is thought to be the diastereomeric LIM-18A branched acyl complex, **7**. Also observed is a broad peak at ~26 ppm attributed to the hydride species, $[HCo(CO)_3(LIM\text{-}18B)]$.[7]

Increasing the temperature to 80 °C (Fig. 3d), accelerates the conversion of the terminal acyl species, **5**, to $[Co_2(CO)_7(LIM\text{-}18)]$ and $[Co(CO)_3(LIM\text{-}18)]_2$. The resonance for the LIM-18B branched acyl complex, **7**, is believed to overlap with that from the LIM-18A terminal acyl complex, **5**, with all three peaks from the various acyl species being of similar intensity. The solution was then left to cool to room temperature and allowed to equilibrate over 90 min. A subsequent spectrum (Fig. 3e) shows almost complete conversion to $[Co_2(CO)_7(LIM\text{-}18)]$ and $[Co(CO)_3(LIM\text{-}18)]_2$. Traces of of hydride (26.9 ppm) and the acyl complexes, **5** (20.6, 18.6 ppm), are also present along with the branched acyl species, **7** (21.3, 19.5 ppm). The other small peaks between 20.7 and 18.6 ppm may possibly be from branched acyl isomers at the C_3 position.

Infrared analysis of the reaction products supports the conclusions drawn from the NMR experiments. Prior to the addition of syngas, the cobalt acyl complex, **5**, is clearly visible with ν_{CO} at 2039 and 1969 and a characteristic acyl $\nu_{C=O}$ band of medium intensity at 1679 cm^{-1}. After the addition of syngas and heating to 80 °C, the only stretches observed are those of the monophosphine dimeric species $[Co_2(CO)_7(LIM\text{-}18)]$ and $[Co(CO)_3(LIM\text{-}18)]_2$.

If the species resonating at 21.2 and 19.5 ppm are the (4*R,S*)-branched acyl complexes, **6**, it implies that, in the presence of H_2/CO and at temperatures below 100 °C, the rate of hydrogenolysis of the terminal acyl complex is slow enough to allow for the interconversion to the alkyl complex followed by β-hydride elimination to form the alkene complex, remigration of H and remigration of the branched alkyl ligand onto CO, as shown in Scheme 2. It is known that alkene isomerisation in these complexes occurs at a much faster rate than hydro-

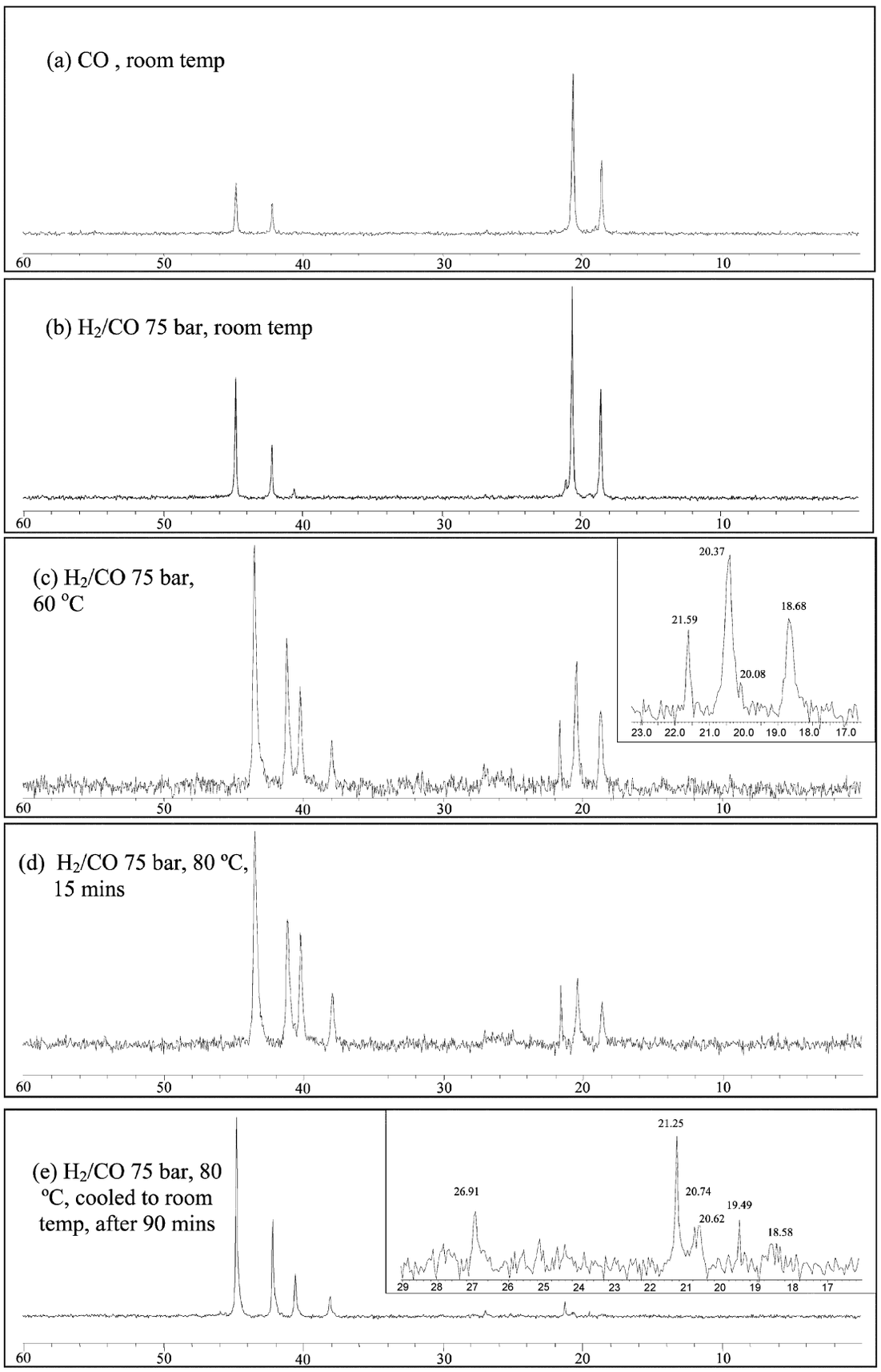

Fig. 3 ^{31}P NMR studies of [Co(hexanoyl)$(CO)_3$(LIM-18)].

formylation, even under reaction conditions (85 bar, 180 °C). Although it seems unlikely that this isomerisation involves acyl intermediates, it is highly probable that if the alkyl group does migrate from CO to Co, the reformed acyl complex will have the acyl group on an internal C atom.

Hydroformylation reactions

Having separated the two diastereomers of LIM-18, it was of interest to know whether they would differ in terms of activity or selectivity in hydroformylation reactions. Hydroformylation

Table 4 Cobalt/LIM catalysed hydroformylation of 1-octene at 85 bar H_2:CO (2:1)

Expt.	Ligand	*t*/h	*T*/°C[a]	Residual alkene (%)	n-Octane (%)	Aldehyde (%)	Unknown[b] (%)	Branched alcohol[c] (%)	1-Nonanol	l:b[d]	Rate const./ h^{-1}
1	LIM-18	6	174.8	1.3	7.7	0.4	10.5	18.5	61.7	3.3 (5.5)	0.84
2	LIM-18	6	174.5	0.6	7.2	0.4	4.2	24.9	63.0	2.5 (4.2)	0.85
3	LIM-18	7	170.0	2.8	6.6	0.7	4.2	19.6	66.1	3.4 (5.5)	0.59
4	LIM-18	6	172.0	1.9	6.4	0.6	4.3	21.1	65.8	3.1 (5.1)	0.69
5 (MD)[e]	LIM-18B	6	175.5	0.9	6.7	0.3	3.4	27.9	60.8	2.2 (3.7)	0.86
6	LIM-$CH(C_{10}H_{21})_2$	6	171.0	1.1	7.6	0.8	2.8	31.2	56.6	1.8 (3.0)	1.06
7	LIM-$CH(C_{10}H_{21})_2$	7	173.0	0.5	7.3	0.5	3.6	31.4	56.7	1.8 (3.0)	1.05
8	LIM-Bu^t	6	171.0	3.4	8.3	1.6	4.2	20.1	62.5	3.1 (5.2)	—[f]
9	LIM-Bu^t	7	170.5	3.3	8.3	1.2	4.7	19.6	62.9	3.2 (5.3)	—[f]
10	PBu_3	10	170.0	28.6	11.7	2.9	8.1	6.4	42.3	6.6 (9.7)	0.15
11	PBu_3	7	190.5	4.3	16.5	0.4	13.0	10.3	55.5	5.4 (8.6)	0.54

[a] Temperature is ±0.5 °C. [b] There is 1 major unknown product. The GCMS of this product is virtually identical to that of 1-nonanol but it is ***not*** 2-, 3-, 4- or 5-nonanol. However, it does appear to be some isomeric form of $C_9H_{20}O$. [c] Sum of 2-methyloctanol + 2-ethylheptanol + 2-propylhexanol. [d] Ratio: 1-nonanol/sum of (2-methyloctanol, 2-ethylheptanol and 2-propylhexanol). Figure in brackets: 1-nonanol/2-methyloctanol. [e] Major diastereomer of (4*R*)-LIM-18. [f] Consistent, but complex, kinetics of gas uptake.

of a 50% solution of 1-octene in decane was carried out under CO–H_2 (85 bar) at 170 °C using Co:P of 1:4. The major products were 1-nonanol and 2-methyloctanol. Minor products included 2-ethylheptanol and 2-propylhexanol from hydroformylation of isomerised octenes, the hydrogenation product, octane, (up to 8%) and trace amounts of aldehyde. In all experiments an unknown isomeric form of $C_9H_{22}O$ was detected but not identified.

A mixture of the two diastereomers, LIM-18A and B (55:44) was used as ligand in experiments 1–4 (Table 4). Under the reaction conditions, most of the cobalt is complexed by LIM-18A. Averaging the results produces a l:b ratio of ~3.1 with a rate constant of 0.74 h^{-1}. When the reaction was repeated using a sample enriched in LIM-18B, (>96%, Expt. 5) the rate was not greatly altered (0.86 h^{-1}), whilst the l:b ratio was reduced somewhat (2.2). These results suggest that there are no great differences between the two diastereomers in promoting selectivity, but that the weaker coordinating power of LIM-18B means that more cobalt complex containing no bound phosphine is present. It has been shown that when larger concentrations of unliganded cobalt complex are present, these reactions lead to higher rates and lower l:b ratios.[7]

When the primary C-18 alkyl chain was replaced by a secondary $CH(C_{10}H_{21})_2$ alkyl chain (Expts. 6 and 7), the rate was increased (1.06 h^{-1}) and the selectivity reduced (~1.8), as expected for the much bulkier and presumably more weakly coordinating phosphine.

Interestingly, hydroformylation using a bulky tertiary butyl modified ligand (Expts. 8 and 9) demonstrated both a good l:b ratio of ~3.2 and an efficient rate, but also an increased rate of alkene hydrogenation. These results suggest that less unliganded cobalt complex is present in this system, perhaps because the Bu^t group, despite its tertiary centre attached to P, is sterically less demanding than LIM-18 with its primary centre, but much longer chain. Using the X-ray crystallographic data, we have measured the Tolman cone angle for the two ligands in $[Co_2(CO)_6(LIM\text{-}18A)_2]$, as well as the two ligands in a ruthenium complex of LIM-18A. The four ligands have cone angles of 140, 126, 139 and 126°. We have then replaced the $C_{18}H_{37}$ chains in each ligand by an idealised Bu^t group and remeasured the Tolman cone angles as 124, 116, 124 and 116° respectively. The important observation is that in each case, the cone angle for the Bu^t derivatised ligand is some 10–16° **smaller** than that for Lim-18A itself confirming that the Bu^t derivatised ligand is less sterically demanding. Although the gas uptake when using LIM-Bu^t was observed to be similar to that of experiments 6 and 7, the kinetics were not first order and hence a true rate constant could not be determined. The importance of steric effects is further demonstrated by a comparison with reactions carried out using PBu_3 as a ligand (Expts. 10 and 11). The lower reaction rate and higher l:b ratio, as well as the increase in alkane formation confirm that less unliganded cobalt is present in this system, despite the anticipated poorer electron donating properties of this small ligand.

Conclusion

Using the preferential coordination of one diastereomer of LIM-18 to cobalt, we have succeeded in synthesising complexes enriched in one or other of the diastereomers and hence in assigning their spectra. On the basis of modelling and preferential reactivity, we conclude that the (4*R*) isomer, despite being slightly less basic, binds more strongly to cobalt as steric constraints dominate. A complex containing the (4*R*) isomer has been characterised crystallographically. The enriched LIM-B (believed to be (4*S*)), shows similar activity and selectivity to the mixture of isomers in hydroformylation reactions. The important acyl intermediate reductively eliminates aldehyde under CO/H_2, but also appears to undergo competitive isomerisation of the alkyl chain. Bulky secondary alkyl groups on the P atom of the LIM skeleton give catalytic results indicative of less coordinated cobalt being present, but Bu^t on the P atom appears to give slightly better selectivity than LIM-18, perhaps suggesting that the primary C_{18} chain is bulkier than the tertiary-butyl group.

Experimental

Microanalyses were performed by the University of St. Andrews Microanalytical Service. Infrared spectra were obtained using a Nicolet Protégé 460 FT spectrometer with CsI optics interfaced to a personal computer *via* the OMNIC operating system. ^1H, ^{13}C and ^{31}P NMR spectra were recorded on a Bruker AM 300 or a Varian Gemini 300 spectrometer with broadband proton decoupling for ^{13}C and ^{31}P nuclei. ^1H and ^{13}C NMR spectra were referenced internally to deuterated solvents, which were referenced relative to TMS at $\delta = 0$. ^{31}P NMR spectra were referenced externally to phosphoric acid 85% H_3PO_4. Coupling constants are given in Hertz.

Manipulations were carried out under dry oxygen free nitrogen or argon using Schlenk techniques or a drybox. All solvents were freshly distilled and dried; petroleum ether (boiling range, 40–60 °C), tetrahydrofuran and diethylether were distilled over sodium diphenylketyl, toluene over sodium, dichloromethane and cyclohexane were distilled over calcium hydride. All gases

were purchased from BOC and used without further purification.

$[Co_2(CO)_8]$ was purchased from Aldrich and recrystallised from pentane before use. The ligands 4,8-dimethyl-2-phospha-bicyclo[3.3.1]nonane and 4,8-dimethyl-2-octadecyl-2-phospha-bicyclo[3.3.1]nonane were procured from Cytech Canada Inc. and used without further purification.

2-(1-Decyl-undecyl)-4,8-dimethyl-2-phospha-bicyclo[3.3.1] nonane [LIM-CH($C_{10}H_{21}$)$_2$]

An ethereal solution of decylmagnesium bromide formed by the Grignard reaction of 1-bromodecane (10.0 g, 45.27 mmol) and magnesium turnings (2.2 g), was filtered into a solution of undecanal (7.70 g, 45.29 mmol) at 0 °C with stirring. Disappearance of the aldehyde and formation of the secondary alcohol heneicosan-11-ol was monitored by thin layer chromatography, staining with potassium permanganate solution. On completion of the reaction, the mixture was quenched with water then extracted, dried ($MgSO_4$) and recrystallised with dichloromethane. Regioselective bromination of the isolated secondary alcohol was achieved using an *in situ* preparation of PPh_3Br_2 in DMF. The dry alcohol (1.00 g, 3.20 mmol) was stirred with PPh_3 (0.92 g, 3.51 mmol) in dry dimethylformamide (20 mL) under an argon atmosphere. Bromine was then added dropwise over a 15 min period while the flask was kept below 55 °C. The addition was stopped when two drops persisted in giving an orange colour to the solution. Removal of the solvent followed by recrystallization of the crude product with dichloromethane afforded 11-bromoheneicosane in sufficient purity for use in the next stage of the reaction. The reaction of the secondary halo-alkane (0.106 g, 0.28 mmol) with lithium 4,8-dimethyl-2-phosphido-bicyclo[3.3.1]nonane (Li[$PC_{10}H_{18}$]) (0.050 g, 0.28 mmol) (formed *in situ* from 4,8-dimethyl-2-phospha-bicyclo[3.3.1]nonane ($HPC_{10}H_{18}$) and an equimolar amount of Bu^nLi in THF) was conducted at 0 °C and the mixture was then left to stir overnight. The solvent was removed *in vacuo* and the crude product redissolved in petroleum ether (30 mL). Degassed water (40 mL) was added, the layers separated and the organic layer dried using $MgSO_4$. Concentration of the product followed by Kugelrohr distillation (125 °C, 0.1 mm Hg) to remove impurities yielded the product [LIM-CH($C_{10}H_{21}$)$_2$] as an air sensitive viscous oil ^{31}P NMR ($CDCl_3$, 121.5 MHz) δ −36.1, −42.1 ppm. It was used without further purification.

2-(t-butyl)-4,8-dimethyl-2-phospha-bicyclo[3.3.1]nonane [LIM-Bu^t]

[LIM-Bu^t] was similarly prepared by the metathetical reaction of ^{t}BuCl (2.59 g, 0.35 mmol) with lithium 4,8-dimethyl-2-phosphido-bicyclo[3.3.1]nonane, Li[$PC_{10}H_{18}$] (0.32 mmol). The crude product was isolated as above and purified by Kugelrohr distillation (85 °C, 0.1 mmHg) yielding the product LIM-Bu^t which was used without further purification. ^{31}P NMR ($CDCl_3$, 121.5 MHz) δ −36.5, −42.5 ppm.

Isolation of LIM-18B

Under a carbon monoxide atmosphere, $[Co_2(CO)_8]$ (2.00 g, 5.85 mmol) was dissolved in light petroleum (40 mL) and cooled to 0 °C. With rapid stirring, a solution of LIM-18 (7.42 g, 17.58 mmol) dissolved in light petroleum (20 mL) was then added. On addition of the phosphine, carbon monoxide gas was liberated. Stirring was continued for a further 30 mins at 0 °C followed by standing to allow the salt to separate. The supernatant liquid was then transferred *via* cannula and reduced *in vacuo*. The resulting red oil was dissolved in a minimum of dichloromethane and loaded onto a silica column under argon. Elution with 100% dichloromethane removed a fast flowing red/brown band close to the solvent front (dimeric cobalt species). Subsequent elution with 100% diethyl ether and removal of solvent liberated LIM-18B in 96% purity. ^{31}P NMR: δ −51.8 ppm.

Enrichment of [Co(CO)$_3$(LIM-18A)$_2$][Co(CO)$_4$]

Under a carbon monoxide atmosphere, $[Co_2(CO)_8]$ (0.50 g, 1.46 mmol) was dissolved in light petroleum (40 mL) and cooled to 0 °C. With rapid stirring, a solution of LIM-18 (3.70 g, 8.77 mmol) dissolved in light petroleum (20 mL) was added. On addition of the phosphine, carbon monoxide gas was liberated. Stirring was continued for a further 30 min at 0 °C followed by standing to allow the salt to separate. The organic layer was decanted *via* cannula and the resulting deep red viscous salt was washed with cold pentane (20 mL) three times and dried *in vacuo*. ^{31}P NMR analysis confirmed enrichment of the $[Co(CO)_3(LIM\text{-}18A)_2][Co(CO)_4]$ salt with the major peak (69%) at δ 37.78 ppm. IR (neat) ν(CO): 2062 (s), 2005 (vs), 1986 (vs), 1948 (s), 1889 (vs) cm^{-1}. Found: C, 65.44, H, 10.06%; $C_{63}H_{110}Co_2O_7P_2$ (M_w = 1159.38) requires C, 65.27, H, 9.56%.

On standing, this oil produced a few crystals, one of which was used for X-ray analysis and shown to be [Co(CO)$_3$((4*R*)-LIM-18)]$_2$.

Note: Subsequent reactions to form the Co/LIM-18 species are identical using enriched LIM-18B or enriched [Co(CO)$_3$-(LIM-18A)$_2$][Co(CO)$_4$] and the complexes have equivalent infrared stretching frequencies, hence only the reaction for the LIM-18A isomer is detailed. The ^{31}P NMR spectra of the different complexes are collected in Table 1.

[Co(CO)$_3$(LIM-18A)$_2$]$_2$

Under an argon atmosphere, $[Co(CO)_3(LIM\text{-}18A)_2][Co(CO)_4]$ (2.05 g, 1.81 mmol) was dissolved in toluene (40 mL) and heated to 90 °C for 2 h to effect decarbonylation of the ionic salt. The solution was then cooled to room temperature and the toluene solvent removed *in vacuo* to give a deep red viscous oil. IR (hexane) ν(CO): 2030 (w), 1968 (s), 1949 (vs), 1924 (w), 1898 (sh, w) cm^{-1}. Found: C, 65.20, H, 10.20%; $C_{62}H_{110}Co_2O_6P_2$ (M_w = 1131.37) requires C, 65.82, H, 9.80%. Attempts at obtaining spectra at low temperature were frustrated by precipitation of the compound.

[Co$_2$(CO)$_7$(LIM-18A)]

$[Co_2(CO)_8]$ (0.62 g, 1.81 mmol) was dissolved in petroleum ether at room temperature and added to a carbon monoxide purged solution of the disubstituted dimer $[Co(CO)_3(LIM\text{-}18A)]_2$ (2.05 g, 1.81 mmol) in petroleum ether (20 mL). Carbon monoxide was then bubbled through the reaction mixture which was monitored by infrared spectroscopy for the disappearance of the stretch at 1949 cm^{-1} and the subsequent appearance of stretches for the substituted monophosphine dimer at 2077 cm^{-1} and 1992 cm^{-1}. IR (hexane) ν(CO): 2077 (s), 2021 (s), 1992 (vs), 1953 cm^{-1} (m).

[HCo(CO)$_3$(LIM-18)]

LIM-18 (20 mg, 0.047 mmol) dissolved in deuteriated benzene (1 mL) was added to a stirred solution of $[Co_2(CO)_8]$ (81 mg, 0.237 mmol) in d_6-benzene (1 mL). The reaction mixture was then transferred to a 40 mL stainless steel autoclave which was then charged with syngas (H_2 : CO, 1 : 1) to a pressure of 66 bar. The autoclave was heated to 170 °C for 2 h with stirring and then quickly cooled to room temperature using iced water. The contents were immediately transferred under argon and characterised by NMR and infrared spectroscopy. ^{31}P NMR ($CDCl_3$): $HCo(CO)_3(LIM\text{-}18A)$ δ = 26.9, $HCo(CO)_3(LIM\text{-}18B)$ δ = 28.5 ppm. IR (C_6D_6) ν(CO): 2077 (s), 2021 (s), 1992 (vs), 1953 cm^{-1} (m).

[CH$_3$(CH$_2$)$_4$COCo(CO)$_3$(LIM-18)]

The preparation of the acyl complex was similar to those found in literature.[10,11] Hexanoyl chloride (0.39 g, 2.92 mmol) was added dropwise to an ethereal solution of Na[Co(CO)$_4$]

(formed *in situ* from $Co_2(CO)_8$ (0.50 g, 1.46 mmol) and 5% NaHg amalgam stirred vigorously in THF) at 0 °C and left to stir for 1–2 h until the characteristic tetracarbonyl band at 1890 cm^{-1} disappeared. The suspension was filtered and the filtrate stirred with an equimolar amount of LIM-18 (1.23 g, 2.92 mmol) at room temperature for two hours. The solvent was evaporated under reduced pressure to yield a red oil, which was readily soluble in organic solvents. ^{31}P NMR (d_8-toluene): $[CH_3(CH_2)_4COCo(CO)_3$(LIM-18A)] δ = 20.6, $[CH_3(CH_2)_4$-$COCo(CO)_3$(LIM-18B)] δ = 18.5 ppm. IR (hexane) ν(CO): 2039 (m), 1969 (s), 1947 (s), 1679 (m) cm^{-1}

Measurements of equilibrium constant ratios for reactions of LIM-18A and LIM-18B with Me^+, H^+ and $[Co_2(CO)_8]$

Quantities (*ca.* 100 mg) of LIM-18 were weighed out accurately into Schlenk tubes in a glove box and then moved to a fume cupboard. A 1 : 4 mixture of d^6-acetone/acetone (1 mL) was added and aliquots of CF_3SO_3Me corresponding to approximately 20, 40, 60 and 80% were added under nitrogen. After stirring for 30 min, the solutions were transferred to NMR tubes under nitrogen. The ^{31}P NMR spectra of the solutions were recorded and the ratio of equilibrium constants (K_A/K_B) was obtained for each solution from integration of the spectra, using the following equation:

$$K_A/K_B = (AMe^+)(B)/(BMe^+)(A)$$

where A, B, AMe^+ and BMe^+ are the integrals for the signals from LIM-18A, LIM-18B and their methylated forms respectively. The use of this equation is based on the assumption that the receptivities of the isomer pairs LIM-18A and LIM-18B and LIM-18AMe^+ and LIM-18BMe^+ are the same, but does not assume that the receptivities of other components (*e.g.* LIM-18A and LIM-18AMe^+) are necessarily the same.

Similar procedures were used in the corresponding measurements with $[Co_2(CO)_8]$ (1 : 4 d_6-benzene/toluene) and *p*-toluenesulfonic acid (in 1 : 4 d^6-acetone/acetone), except that those for the latter were carried out at 0 °C. The equation used for the protonation calculation is analagous to that above (with AH^+ rather than AMe^+ etc.). That used for the cobalt complexation experiment is given below:

$$K_A/K_B = (CoA)(B)^2/(CoB)(A)^2$$

where A, B, CoA and CoB are the integrals for the signals from LIM-18A, LIM-18B, and the complexes $[Co(CO)_3$(LIM-18A)$]_2$ and $[Co(CO)_3$(LIM-18B)$]_2$, respectively.

Catalytic reactions

Kinetic studies were performed using a 30 mL reaction vessel fitted with a substrate injection facility, overhead mechanical stirrer, thermocouple, pressure gauge and a high pressure synthesis gas reservoir or ballast vessel. In a typical reaction, a clear, colourless pre-prepared decane solution of LIM-18 (1.25 mL, 0.253 mmol) was added to the autoclave followed by a clear, dark red pre-prepared decane solution of $[Co_2(CO)_8]$ (1.25 mL, 0.032 mmol) under a CO/H_2 (1 : 2) flush. The combined solution was flushed with 3 cycles of *ca.* 20 bar of CO/H_2 (1 : 2) while being stirred. After flushing was completed, the autoclave was pressurised to *ca.* 60 bar, sealed and heated to *ca.* 170 °C. Once the temperature had stabilised and the catalyst had formed (approximately 1 h), 1-octene (2.5 mL) was injected. The pressure was increased to 85 bar and maintained constant by feeding gas from the ballast vessel through a mass flow controller. The pressure drop in the ballast vessel was electronically monitored and plotted. The reaction was run for 6 h in total, at which point the gas uptake had virtually ceased. These proportions give 1000 ppm w/w of Co in solution with a 1 : 4 Co : P ratio. Oct-1-ene : decane 50/50 by volume.

High pressure NMR studies

The complex $[CH_3(CH_2)_4COCo(CO)_3$(LIM-18)] (100 mg) was dissolved in toluene containing d_8-toluene and transferred to a 10 mm sapphire NMR tube fitted with a pressure head. The tube was pressurised with a mixture of CO/H_2 1 : 1 (75 bar). The ^{31}P NMR spectrum was recorded at room temperature, 60 °C and finally at 80 °C at which temperature it was left to equilibrate for 15 min. The sample was cooled back to room temperature and a final spectrum was recorded after 90 min.

X-ray crystal and molecular structure of $[Co_2(CO)_6$((1-*R*,4-*R*, 5-*R*,8-*S*)-LIM)$_2]$§

X-ray diffraction measurements were made with graphite-monochromated Mo-Kα X-radiation (λ = 0.71073 Å) using a Bruker SMART diffractometer, intensity data were collected using 0.3° width ω steps accumulating area detector frames spanning a hemisphere of reciprocal space (data were integrated using the SAINT program). Data were corrected for Lorentz, polarisation and long-term intensity fluctuations. Absorption effects were corrected on the basis of multiple equivalent reflections or by semi-empirical methods. Structures were solved by direct methods and refined by full-matrix least-squares against F^2 (SHELXTL). All hydrogen atoms were assigned isotropic displacement parameters and were constrained to idealised geometries. The alkyl chains were refined with fixed geometry. The alkyl chains and carbonyls were refined isotropically. Refinements converged to residuals given in Table 4. All calculations were made with SHELXTL.[17]

CCDC reference number 218353.

See http://www.rsc.org/suppdata/dt/b3/b310233e/ for crystallographic data in CIF or other electronic format.

Molecular modelling

All geometry optimizations were performed with the DMol^3 Density Functional Theory (DFT) code[18–20] as implemented in the MaterialsStudio™ (Version 2.1.5) program package of Accelrys Inc.[21] on SGI and Compaq Alpha workstations. DMol^3 uses numerical orbitals for the basis functions as opposed to analytical functions (*i.e.* Gaussian type orbitals). In this study the double numerical basis set (DNP) containing a p-polarization function for H and d-polarization functions for other atoms were used. The DNP basis set was chosen because it is equivalent in quality and size to the Gaussian 6-31G** split-valence double-zeta plus polarization basis set. The latter is generally accepted as the standard basis set in Hartree Fock (HF) quantum calculations. The generalized gradient approximation (GGA) functional by Perdew and Wang (PW91)[22] was used for all geometry optimisations. The convergence criteria for these optimisations consisted of threshold values of 2×10^{-5} Ha, 0.00189 Ha $Å^{-1}$ and 0.00529 Å for energy, gradient and displacement convergence, respectively, while a self consistent field (SCF) density convergence threshold value of 1×10^{-6} was specified. All calculated reaction energies reported herein are total electronic energies at 0 K of the respective geometries after optimisation.

In the case of LIM-18 and $[HCo(CO)_3$(LIM-18)], an annealing dynamics protocol, involving 200 steps of dynamics, a time step of 0.0005 ps, an initial temperature of 200 K, a midcycle

§ *Crystal data* for $Co_2(CO)_6$(LIM-18)$_2$: $Co_2C_{62}H_{110}O_6P_2$, M = 1131.35, orthorhombic, $P2_12_12_1$, a = 8.8894(3), b = 12.6610(3) c = 60.1359(3) Å, V = 6768.2(3) $Å^3$ Z = 4, μ(Mo-Kα) = 0.58 mm^{-1} T = 293 K, SMART diffractometer, of 29519 reflections measured 9604 were independent (R_{int} = 0.0763) to give R = 0.105 for 4474 observed reflections, [$I > 2\sigma(I)$], Flack parameter = 0.10(5).

temperature of 2000 K and a temperature increment of 200 K, was followed to yield the most stable conformers. The dynamics were performed with the anneal molecular dynamics functionality incorporated in the Accelrys Cerius[2] (Version 4.6) program[21] suite, using the universal force field (UFF)[23–25] The trigonal bipyrimidal arrangement of the Cobalt metal centre was constrained during the MD runs due to the lack of appropriate force field parameters for Co and the said geometry.[7]

After each MD run the ten most stable conformers were subjected to a full geometry optimisation with the Semi Empirical (SE) PM3 method[26] as incorporated in the Spartan '02 for Unix program package available from Wavefunction[27] The conformer with lowest SE/PM3 predicted total electronic energy was used for consequent DFT geometry optimisation as described above. This procedure was followed to ensure that global minima structures for both ligand and complex structures were obtained. For the purpose of this comparative study only the global energy minimum structures are important and although the mentioned protocol cannot guarantee global energy minima, it was deemed comprehensive enough to ensure energy values in very close proximity to the required global energy minima.

Acknowledgements

We would like to thank Sasol Technology Ltd. for the generous provision of funding for postdoctoral fellowships (to A. P. and J. D. E. T. W.-E.) and materials.

References

1 C. D. Frohning and C. W. Kohlpaintner, in *Applied Homogeneous Catalysis with Organometallic Compounds*, ed. B. Cornils and W. A. Herrmann, VCH, Weinheim, 1996, vol. 1, p. 27.
2 P. N. W. M. Van Leeuwen and C. Claver, *Rhodium Catalysed Hydroformylation*, Kluwer, 2000.
3 J. L. van Winkle, S. Lorenzo, R. C. Morris and R. F. Mason, *US Patent*, 1969, 3420898.
4 D. Vogt, in *Applied Homogeneous Catalysis with Organometallic Compounds*, ed. B. Cornils and W. A. Herrmann, VCH, Weinheim, 1996, p. 245.
5 J. H. Downing, V. Gee and P. G. Pringle, *Chem. Commun.*, 1997, 1527.
6 J. P. Steynberg, K. Govender and P. J. Steynberg, *World Patent, WO*, 2002, 14248.
7 C. Crause, L. Bennie, L. Damoense, C. L. Dwyer, C. Grove, N. Grimmer, W. J. van Rensburg, M. M. Kirk, K. M. Mokheseng, S. Otto and P. J. Steynberg, *Dalton Trans.*, 2003, 2036.
8 A. Robertson, C. Bradaric, C. S. Frampton, J. McNulty and A. Capretta, *Tetrahedron Lett.*, 2001, **42**, 2609.
9 K. W. Kramarz, R. J. Klingler, D. E. Fremgen and J. W. Rathke, *Catal. Today*, 1999, **49**, 339.
10 Although 16 diastereomers are possible when there are 4 stereogenic centres, the use of (*R*)-(+)-limonene reduces this number to eight.
11 R. F. Bryan and A. R. Manning, *J. Chem. Soc., Chem. Commun.*, 1968, 1316.
12 J. A. Ibers, *J. Organomet. Chem*, 1968, **14**, 423.
13 J. Andzelm, K. Glassford, N. Govind, G. Fitzgerald and K. Stark, ACS, 2002, Orlando; A. Scheiner, J. Baker and J. Andzelm, *J. Comput. Chem.*, 1997, **18**, 775.
14 F. Axe and J. Andzelm, *J. Am. Chem. Soc.*, 1999, **121**, 5396.
15 R. F. Heck and D. S. Breslow, *J. Am. Chem. Soc.*, 1962, **84**, 2499.
16 E. Lindner and M. Zipper, *Chem. Ber.*, 1974, **107**, 1444.
17 G. M. Sheldrick, SHELXTL, Bruker AXS, 1999.
18 B. Delley, *J. Chem. Phys.*, 2000, **113**, 7756 and references therein.
19 B. Delley, *J. Phys. Chem.*, 1996, **100**, 6107.
20 B. Delley, *J. Chem. Phys.*, 1990, **92**, 508.
21 http://www.accelrys.com.
22 J. P. Perdew, *Phys. Rev. B*, 1986, **33**, 8822.
23 A. K. Rappe, K. S. Colwell and C. J. Casewit, *Inorg. Chem.*, 1993, **32**, 3438.
24 A. K. Rappe, C. J. Casewit, K. S. Colwell, W. A. Goddard and W. M. Skiff, *J. Am. Chem. Soc.*, 1992, **114**, 10024.
25 C. J. Casewit, K. S. Colwell and A. K. Rappe, *J. Am. Chem. Soc.*, 1992, **114**, 10035.
26 J. J. P. Stewart, *J. Comput. Chem.*, 1989, **10**, 209.
27 http://www.wavefun.com.